

## $\Lambda$ and $\bar{\Lambda}$ reconstruction in central Pb + Pb collisions using a time projection chamber

T Yates and the NA49 Collaboration

S V Afanasiev<sup>9</sup>, T Alber<sup>13</sup>, H Appelshäuser<sup>7</sup>, J Bächler<sup>5</sup>, S J Bailey<sup>16</sup>,  
 L S Barnby<sup>3</sup>, J Bartke<sup>6</sup>, H Białkowska<sup>14</sup>, C O Blyth<sup>3</sup>, R Bock<sup>7</sup>,  
 C Bormann<sup>10</sup>, F P Brady<sup>8</sup>, R Brockmann<sup>7</sup>, N Buncic<sup>5,10</sup>, P Buncic<sup>5,10</sup>,  
 H L Caines<sup>3</sup>, D Cebra<sup>8</sup>, P Chan<sup>16</sup>, G E Cooper<sup>2</sup>, J G Cramer<sup>16,13</sup>,  
 P B Cramer<sup>16</sup>, P Csato<sup>4</sup>, O Dietz<sup>10</sup>, J Dunn<sup>8</sup>, V Eckardt<sup>13</sup>, F Eckhardt<sup>12</sup>,  
 M I Ferguson<sup>5</sup>, H G Fischer<sup>5</sup>, D Flierl<sup>10</sup>, Z Fodor<sup>4</sup>, P Foka<sup>7,10</sup>, P Freund<sup>13</sup>,  
 V Friese<sup>12</sup>, M Fuchs<sup>10</sup>, F Gabler<sup>10</sup>, J Gal<sup>4</sup>, M Gaździcki<sup>10</sup>, E Gładysz<sup>6</sup>,  
 J Grebieszko<sup>15</sup>, J Günther<sup>10</sup>, J W Harris<sup>17</sup>, S Hegyi<sup>4</sup>, T Henkel<sup>12</sup>,  
 L A Hill<sup>3</sup>, I Huang<sup>2,8</sup>, M A Howe<sup>16</sup>, H Hümmeler<sup>10</sup>, G Igo<sup>11</sup>,  
 D Irmscher<sup>2,7,†</sup>, P Jacobs<sup>2</sup>, P G Jones<sup>3</sup>, K Kadija<sup>18,13</sup>, V I Kolesnikov<sup>9</sup>,  
 M Kowalski<sup>6</sup>, B Lasiuk<sup>11</sup>, P Lévai<sup>4</sup>, A I Malakhov<sup>9</sup>, S Margetis<sup>2,‡</sup>,  
 C Markert<sup>7</sup>, G L Melkumov<sup>9</sup>, A Mock<sup>13</sup>, J Molnár<sup>4</sup>, J M Nelson<sup>3</sup>,  
 G Odyniec<sup>2</sup>, G Palla<sup>4</sup>, A D Panagiotou<sup>1</sup>, A Petridis<sup>1</sup>, A Piper<sup>12</sup>,  
 R J Porter<sup>2</sup>, A M Poskanzer<sup>2,§</sup>, S Poziombka<sup>10</sup>, D J Prindle<sup>16</sup>,  
 F Pühlhofer<sup>12</sup>, W Rauch<sup>13</sup>, J G Reid<sup>16</sup>, R Renfordt<sup>10</sup>, W Retyk<sup>15</sup>,  
 H G Ritter<sup>2</sup>, D Röhrich<sup>10</sup>, C Roland<sup>7</sup>, G Roland<sup>10</sup>, H Rudolph<sup>2,10</sup>,  
 A Rybicki<sup>6</sup>, I Sakrejda<sup>2</sup>, A Sandoval<sup>7</sup>, H Sann<sup>7</sup>, A Yu Semenov<sup>9</sup>,  
 E Schäfer<sup>13</sup>, D Schmiscke<sup>10</sup>, N Schmitz<sup>13</sup>, S Schönfelder<sup>13</sup>, P Seyboth<sup>13</sup>,  
 J Seyerlein<sup>13</sup>, F Sikler<sup>4</sup>, E Skrzypczak<sup>15</sup>, G T A Squier<sup>3</sup>, R Stock<sup>10</sup>,  
 H Ströbele<sup>10</sup>, I Szentpetery<sup>4</sup>, J Sziklai<sup>4</sup>, M Toy<sup>2,11</sup>, T A Trainor<sup>16</sup>,  
 S Trentalange<sup>11</sup>, T Ullrich<sup>17</sup>, M Vassiliou<sup>1</sup>, G Vesztegombi<sup>4</sup>, D Vranic<sup>7,18</sup>,  
 F Wang<sup>2</sup>, D D Weerasundara<sup>16</sup>, S Wenig<sup>5</sup>, C Whitten<sup>11</sup>, T Wienold<sup>2,†||</sup>,  
 L Wood<sup>8</sup>, T A Yates<sup>3</sup>, J Zimanyi<sup>4</sup>, X-Z Zhu<sup>16</sup> and R Zybent<sup>3</sup>

<sup>1</sup> Department of Physics, University of Athens, Athens, Greece

<sup>2</sup> Lawrence Berkeley National Laboratory, University of California, Berkeley, USA

<sup>3</sup> Birmingham University, Birmingham, England

<sup>4</sup> KFKI Research Institute for Particle and Nuclear Physics, Budapest, Hungary

<sup>5</sup> CERN, Geneva, Switzerland

<sup>6</sup> Institute of Nuclear Physics, Cracow, Poland

<sup>7</sup> Gesellschaft für Schwerionenforschung (GSI), Darmstadt, Germany

<sup>8</sup> University of California at Davis, Davis, USA

<sup>9</sup> Joint Institute for Nuclear Research, Dubna, Russia

<sup>10</sup> Fachbereich Physik der Universität, Frankfurt, Germany

<sup>11</sup> University of California at Los Angeles, Los Angeles, USA

<sup>12</sup> Fachbereich Physik der Universität, Marburg, Germany

<sup>13</sup> Max-Planck-Institut für Physik, Munich, Germany

<sup>14</sup> Institute for Nuclear Studies, Warsaw, Poland

<sup>15</sup> Institute for Experimental Physics, University of Warsaw, Warsaw, Poland

† Alexander von Humboldt Foundation (Lynen) Fellow.

‡ Present address: Brookhaven Nation Laboratory, Upton, NY.

§ Alexander von Humboldt Foundation US Senior Scientist Award Recipient.

|| Present address: Physikalisches Institut, Universitaet Heidelberg, Germany.

<sup>16</sup>Nuclear Physics Laboratory, University of Washington, Seattle, WA, USA

<sup>17</sup>Yale University, New Haven, CT, USA

<sup>18</sup>Rudjer Boskovic Institute, Zagreb, Croatia

Received 30 September 1997

**Abstract.** The large acceptance time projection chambers of the NA49 experiment are used to record the trajectory of charged particles from Pb + Pb collisions at 158 GeV per nucleon. Neutral strange hadrons have been reconstructed from their charged decay products. To obtain distributions of  $\Lambda$ ,  $\bar{\Lambda}$  and  $K_s^0$  in discrete bins of rapidity,  $y$ , and transverse momentum,  $p_T$ , calculations have been performed to determine the acceptance of the detector and the efficiency of the reconstruction software as a function of both variables. The lifetime distributions obtained give values of  $c\tau=7.8\pm 0.6$  cm for  $\Lambda$  and  $c\tau=2.5\pm 0.3$  cm for  $K_s^0$ , consistent with data book values.

## 1. Introduction

The NA49 experiment takes data from high-multiplicity central Pb + Pb collisions using a stationary target and a beam energy of 158 GeV per nucleon. The large acceptance detector system shown in figure 1, consisting of time projection chambers (TPC), time-of-flight arrays (TOF) and calorimeters, measures hadronic spectra [1]. The TPCs record the trajectory of charged particles. Using detailed knowledge of the magnetic fields in which VTTPC1 and VTTPC2 are situated, momenta can be calculated. The main TPC is not in a magnetic field; it can perform particle identification using  $dE/dx$  measurements in conjunction with information from the TOF arrays. The large acceptance of the experiment gives the potential to select individual events showing non-statistical fluctuations for further analysis. This subset of events may show enhanced signatures of deconfined quark matter, such as an enhancement of (anti-)strange hadrons [2, 3].

## 2. Reconstruction details

Neutral strange particles are reconstructed from their charged decay products using the following procedure. All charged particle tracks in VTTPC2 that pass a track quality selection cut are extrapolated towards the target and at 2 cm steps the distance between pairs of oppositely charged tracks is calculated. If the distance of closest approach (DCA) in the  $x$  and  $y$  directions is smaller than predetermined values then the pair of tracks may be used as a decay candidate. Simple geometric cuts illustrated in figure 2 are used to remove combinatorial background. This background consists largely of pairs of primary tracks from the target. Close to the target many pairs of primary tracks will pass the DCA cuts and it is this source of background that is removed by the  $z$  cut. By requiring that pairs of tracks are separated at the target plane, background can be reduced further. Table 1 gives the values used for the cuts for VTTPC2. For each decay candidate that passes the cuts, a geometrical nine-parameter fit is performed using the momenta of the daughter tracks ( $2 \times 3$  parameters) and the position of the decay vertex (three parameters). The invariant mass of the parent particle can then be calculated. Particle identification is possible for charged particles entering the main TPC, but not all tracks from VTTPC2 are in the MTPC acceptance. Therefore, the invariant mass of the parent particle is calculated for three decay hypotheses,  $\Lambda \rightarrow p\pi^-$ ,  $\bar{\Lambda} \rightarrow \bar{p}\pi^+$ ,  $K^0 \rightarrow \pi^+\pi^-$  where the identification of the daughter tracks are assumed (see figure 3).

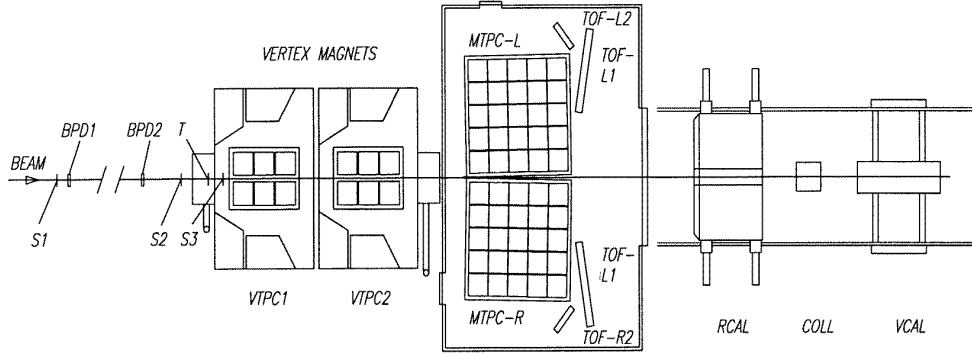


**Figure 1.** A schematic diagram of the NA49 detector system.

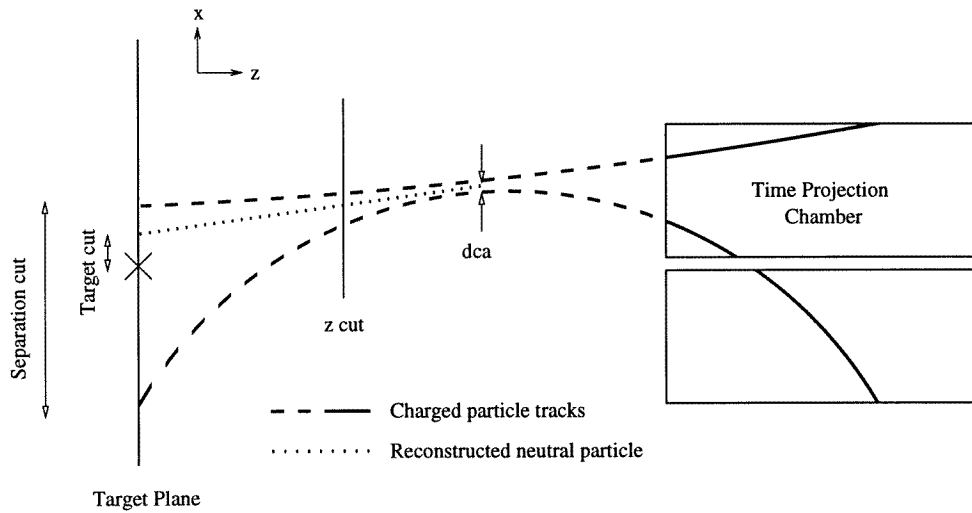


**Figure 2.** Cuts used to remove combinatorial background.

**Table 1.** Cuts used to remove combinatorial background.

Cut	$z$	Separation	Target, $\Delta x$	Target, $\Delta y$	DCA, $x$	DCA, $y$
Value	280.0 cm	5.0 cm	1.11 cm	0.54 cm	1.0 cm	1.0 cm

### 3. Acceptance and efficiency corrections

Corrections for the detector acceptance and reconstruction efficiency are calculated separately, using Monte Carlo (MC) simulated  $\Lambda$ ,  $\bar{\Lambda}$  and  $K^0$  decays. The amount of ionization produced by MC decay products at detectable points along the track is calculated (there are a maximum of 72 detectable points on a track). Using this information it is possible to determine if both decay tracks, and hence the parent particle, are within the acceptance of the detector. By repeating this procedure a large number of times the fraction of acceptable particles can be calculated in discrete bins of  $y$  and  $p_T$ .

A detector response simulator determines the raw data signal that would be produced from the simulated ionization. In order to take account of the high-multiplicity environment,

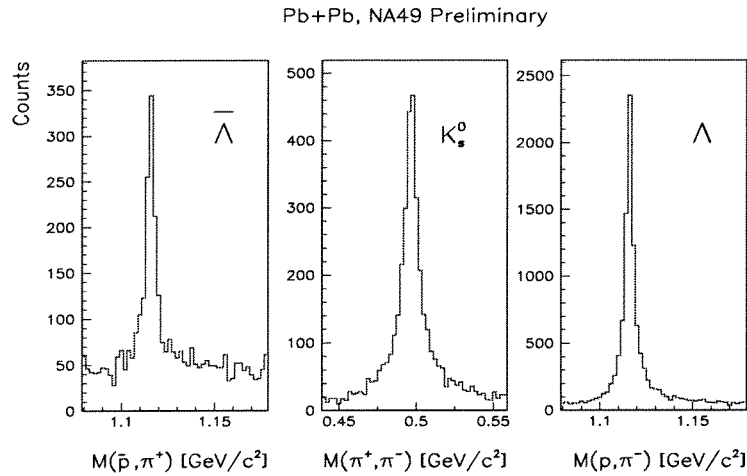


**Figure 3.** Invariant mass distributions for  $\bar{\Lambda}$ ,  $K_S^0$  and  $\Lambda$  from VTPC2.

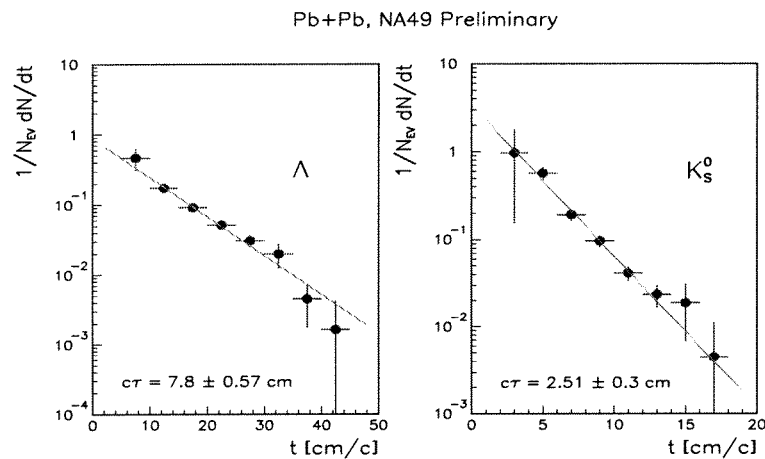


**Figure 4.** Lifetime distributions for  $\Lambda$  and  $K_S^0$  from VTPC2.

the calculation of the reconstruction efficiency is performed by embedding simulated particles into real data at the raw data level. MC decays are only embedded into those events in which no decay candidates were found, so that the MC particle can be identified without ambiguity. Only one MC decay is embedded per event in order to minimize the possibility of perturbing the event.

By re-analysing the events to find the fraction of embedded particles that are reconstructed, it is possible to calculate the reconstruction efficiency, again in discrete bins of  $y$  and  $p_T$ , giving values of  $\sim 40\%$ . A given particle generated in one  $y$ - $p_T$  bin may be reconstructed in another (referred to here as *flow* from one bin to another), due to the finite resolution of the detector. The MC particles were generated with a flat  $y$  and  $p_T$  distribution so as not to assume the distribution of real particles. This results in different amounts of flow in real and MC distributions. Careful account is taken of this flow effect by weighting the flow by the  $y$ - $p_T$  distribution.

Invariant mass distributions in each  $y$ - $p_T$  bin are background subtracted and the resultant yield multiplied by a factor  $1/(\text{acceptance} \times \text{efficiency})$  to obtain  $y$  and  $p_T$  (or transverse mass,  $m_T$ ) distributions [4]. Corrections have not been made for the feeddown  $\Lambda$  from  $\Xi$  decays. A consistency check to ensure that the correction procedure is correct is to plot the lifetime distribution of the particles. Figure 4 shows exponential fits to the data giving values of  $c\tau = 7.8 \pm 0.6$  cm for  $\Lambda$  and  $c\tau = 2.5 \pm 0.3$  cm for  $K_s^0$ , both of which are consistent with data book values at the one sigma level [5].

#### 4. Summary

Using the NA49 experiment VTPC2 detector  $\Lambda$ ,  $\bar{\Lambda}$  and  $K_s^0$  have been reconstructed, using the tracks of their decay products. Using detailed simulation to calculate the detector acceptance and efficiency of reconstruction, the distribution of these particles has been determined in discrete bins of rapidity and transverse momentum. The VTPC1 detector can also be used for the reconstruction of neutral strange particles using the same procedure, but with different geometrical cuts. This detector has high acceptance in a different region to VTPC2, and hence it may be possible to extend the distributions in both  $y$  and  $p_T$ .

#### References

- [1] Afanasiev S V *et al* 1996 *Nucl. Phys. A* **610** 188
- [2] Koch P, Muller B and Rafelski J 1986 *Phys. Rep.* **142** 168
- [3] Sollfrank J and Heinz U 1995 *Quark Gluon Plasma 2* ed R C Hwa (Singapore: World Scientific)
- [4] Bormann C for NA49 Collaboration 1997 *J. Phys. G: Nucl. Part. Phys.* **23** 1817
- [5] Barnett R M *et al* 1996 *Phys. Rev. D* **54** 1